Original Article | Breast Imaging

eISSN 2005-8330
https://doi.org/10.3348/kjr.2019.0568
Korean J Radiol 2020;21(9):1036-1044

Korean Journal of Radiology
KJR

Feasibility Study of Synthetic Diffusion-Weighted MRI in Patients with Breast Cancer in Comparison with Conventional Diffusion-Weighted MRI

Bo Hwa Choi, MD, PhD[1, 2], Hye Jin Baek, MD, PhD[1], Ji Young Ha, MD, PhD[1], Kyeong Hwa Ryu, MD, PhD[1], Jin Il Moon, MD[1], Sung Eun Park, MD, PhD[1], Kyungsoo Bae, MD, PhD[1], Kyung Nyeo Jeon, MD, PhD[1], Eun Jung Jung, MD, PhD[3]

[1]Department of Radiology, Gyeongsang National University School of Medicine, Gyeongsang National University Changwon Hospital, Changwon, Korea; [2]Department of Radiology, National Cancer Center, Goyang, Korea; [3]Department of Surgery, Gyeongsang National University School of Medicine, Gyeongsang National University Changwon Hospital, Changwon, Korea

Objective: To investigate the clinical feasibility of synthetic diffusion-weighted imaging (sDWI) at different b-values in patients with breast cancer by assessing the diagnostic image quality and the quantitative measurements compared with conventional diffusion-weighted imaging (cDWI).

Materials and Methods: Fifty patients with breast cancer were assessed using cDWI at b-values of 800 and 1500 s/mm^2 ($cDWI_{800}$ and $cDWI_{1500}$) and sDWI at b-values of 1000 and 1500 s/mm^2 ($sDWI_{1000}$ and $sDWI_{1500}$). Qualitative analysis (normal glandular tissue suppression, overall image quality, and lesion conspicuity) was performed using a 4-point Likert-scale for all DWI sets and the cancer detection rate (CDR) was calculated. We also evaluated cancer-to-parenchyma contrast ratios for each DWI set in 45 patients with the lesion identified on any of the DWI sets. Statistical comparisons were performed using Friedman test, one-way analysis of variance, and Cochran's Q test.

Results: All parameters of qualitative analysis, cancer-to-parenchyma contrast ratios, and CDR increased with increasing b-values, regardless of the type of imaging (synthetic or conventional) ($p < 0.001$). Additionally, $sDWI_{1500}$ provided better lesion conspicuity than $cDWI_{1500}$ (3.52 ± 0.92 vs. 3.39 ± 0.90, $p < 0.05$). Although $cDWI_{1500}$ showed better normal glandular tissue suppression and overall image quality than $sDWI_{1500}$ (3.66 ± 0.78 and 3.73 ± 0.62 vs. 3.32 ± 0.90 and 3.35 ± 0.81, respectively; $p < 0.05$), there was no significant difference in their CDR (90.0%). Cancer-to-parenchyma contrast ratios were greater in $sDWI_{1500}$ than in $cDWI_{1500}$ (0.63 ± 0.17 vs. 0.55 ± 0.18, $p < 0.001$).

Conclusion: $sDWI_{1500}$ can be feasible for evaluating breast cancers in clinical practice. It provides higher tumor conspicuity, better cancer-to-parenchyma contrast ratio, and comparable CDR when compared with $cDWI_{1500}$.

Keywords: *Breast cancer; b-value; Diffusion-weighted imaging; MRI; Synthetic MRI*

INTRODUCTION

Magnetic resonance imaging (MRI) is widely used for evaluating breast cancer due to its high sensitivity, which can be attributed to its excellent soft-tissue contrast (1). However, breast MRI is a time-consuming modality, as it requires acquisition of multiple sequences. Recently, abbreviated breast MRI protocol was introduced to overcome this issue. However, this technique uses contrast media that can result in unexpected adverse effects (2).

In clinical practice, diffusion-weighted imaging (DWI) may be an alternative approach for evaluating breast lesions,

Received: August 2, 2019 **Revised:** February 20, 2020 **Accepted:** March 17, 2020
Corresponding author: Hye Jin Baek, MD, PhD, Department of Radiology, Gyeongsang National University School of Medicine, Gyeongsang National University Changwon Hospital, 11 Samjeongja-ro, Seongsan-gu, Changwon 51472, Korea.
• E-mail: sartre81@gmail.com

Korean Journal of Radiology
KJR

as contrast agents are not required, and images can be obtained rapidly. Several studies have reported the potential value of DWI as a non-contrast imaging modality in breast cancer detection (3-6). Although the image quality of DWI and apparent diffusion coefficient (ADC) maps are affected by b-value selection, the optimal b-value in breast imaging remains debatable. A large b-value (> 1000 s/mm^2) reflects stronger diffusion-weighting, which suppresses benign and normal tissue and enables detection of cancers (7). However, the limitations of DWI using a high b-value include prolonged acquisition time and low signal-to-noise ratios (SNRs) due to requirement of longer echo times (TEs) and artifacts such as eddy current-induced distortions (8).

In contrast to conventional DWI (cDWI), synthetic DWI (sDWI) is mathematically derived from directly acquired DWI with at least two different b-values (8). This approach may overcome the limitations of cDWI by achieving background suppression of a very high b-value DWI without additional acquisition scan time. Recent studies have reported the clinical usefulness of sDWI in detection of whole-body malignant tumors, hepatic metastases, prostate cancers, cervical cancers, and pancreatic cancers (8-22). To date, few studies have focused on sDWI in breast imaging and have demonstrated excellent lesion conspicuity by suppressing the background signal intensity (SI) in sDWI with high b-values, with consequent improvement in the sensitivity for detection of cancerous lesions (23-25). However, previous studies did not quantitatively evaluate sDWI and cDWI in patients with breast cancer.

Therefore, this study aimed to investigate the clinical feasibility of sDWI at different b-values in patients with breast cancer by qualitative and quantitative assessment compared with cDWI.

MATERIALS AND METHODS

Patient Population

The present study involved retrospective analysis of prospectively acquired data. It was approved by our Institutional Review Board and the need to obtain informed consent was waived. We searched for picture archiving and communication system (PACS) reports. From September 2017 to July 2019, 69 female patients with biopsy-proven breast cancers who underwent preoperative breast 3T MRI were enrolled. We focused on the comparison of sDWI and cDWI with high b-values for detecting breast cancers. Therefore, we selected patients who underwent cDWI at b-values of 800 and 1500 s/mm^2 (cDWI$_{800}$ and cDWI$_{1500}$). We excluded patients who did not undergo cDWI$_{1500}$ (n = 18) and images with poor quality (n = 1). Finally, 50 patients were included in this study (median age, 52.5 years; range, 27–78 years). Histopathological diagnosis was established by ultrasound-guided core needle biopsy (n = 49) or stereotactic biopsy (n = 1). Characteristics of the patients and breast cancers are shown in Table 1. Among the 50 lesions, 41 were surgically removed at our institution. The average size of the lesions measured on pathological specimens was 29.8 ± 19.7 mm (range: 6–100 mm). Nine patients underwent surgery at another hospital. Therefore, we could not measure the pathological size of the lesions in these patients. The histopathological diagnoses included 39 invasive carcinomas

Table 1. Characteristics of 50 Women with Histopathologically-Proven Breast Cancer

Clinical, Radiological and Histopathological Characteristics	Women with Breast Cancer (n = 50)
Patient age, median (range) (years)	52.5 (27–78)
Amount of fibroglandular tissue, no. (%) of patients	
a	2 (4.0)
b	5 (10.0)
c	35 (70.0)
d	8 (16.0)
Background parenchymal enhancement, no. (%) of patients	
Minimal	29 (58.0)
Mild	13 (26.0)
Moderate	4 (8.0)
Marked	4 (8.0)
Menopausal status	
Premenopausal	21 (42.0)
Postmenopausal	29 (58.0)
Histopathological subtype, no. (%) of cancer	
Invasive carcinoma of no special type	28 (56.0)
Invasive carcinoma with medullary feature	5 (10.0)
ILC	2 (4.0)
Mucinous carcinoma	2 (4.0)
Tubular carcinoma	1 (2.0)
Papillary carcinoma	1 (2.0)
DCIS	11 (22.0)
Stage of cancer, no. (%) of patients (n = 41)*	
DCIS	9 (22.0)
Invasive, stage I	16 (39.0)
Invasive, stage II	7 (17.1)
Invasive, stage III	8 (19.5)
Invasive, stage IV	1 (2.4)

*Of 50 lesions, 41 were surgically removed. DCIS = ductal carcinoma *in situ*, ILC = invasive lobular carcinoma

https://doi.org/10.3348/kjr.2019.0568

and 11 ductal carcinomas *in situ*. The median interval between MRI and surgery was 7 days (range, 1–37 days).

Image Acquisition

Breast MRI was performed using a 3T system (Architect, GE Healthcare, Milwaukee, WI, USA) with an 8-channel breast coil in prone position. The following MRI sequences were acquired: 1) 3-dimensional (3D) axial Dixon-based fat-suppressed T2-weighted fast-spin-echo sequence, 2) dynamic contrast-enhanced (DCE) high temporal and spatial resolution 3D T1-weighted sequence (Differential Subsampling with Cartesian Ordering) with dual-echo 3D spoiled gradient echo sequence with Dixon fat-water separation methods, 3) echo-planar imaging (EPI)-based cDWI with b-values of 100 and 800 s/mm^2 (repetition time [TR], 3920 ms; TE, 70.9 ms; number of excitations [NEX], 2 and 6; and acquisition time, 3 minutes 16 seconds) and b-value of 1500 s/mm^2 (TR, 4131 ms; TE, 82.5 ms; NEX, 2 and 6; and acquisition time, 2 minutes 27 seconds). Other parameters were identical between the two b-value acquisitions (section thickness, 5.0 mm; interslice gap, 0.5 mm; slice number, 38; field of view, 340 x 272 mm; and matrix, 128 x 128). The diffusion gradients were applied equally along the read, slice, and phase orthogonal directions. The TEs were set to minimum and were different for different b-values. An inversion preparation pulse with inversion time of 248 ms was applied to reduce fat.

To synthesize DWI at b-values of 1000 and 1500 s/mm^2 ($sDWI_{1000}$ and $sDWI_{1500}$), the following procedure was performed pixel by pixel. The signals of the acquired DWI at b-values of 100 and 800 s/mm^2 were converted to the logarithmic scale and ADC was calculated using a linear least square fitting of the logged signals. Subsequently, the logged signal at b-values of 1000 or 1500 s/mm^2 was calculated by extrapolation of the ADC fitted curve and converted to the final signal at b-values of 1000 or 1500 s/mm^2. The sDWI data were reconstructed using commercially available software MAGiC DWI on a 64-bit Advantage Workstation (GE Healthcare). No errors were logged during processing and the average processing time was approximately under 5 seconds per case. The specific parameters of other sequences and contrast medium administration for MRI are described in the Supplementary Materials.

Image Analyses

For qualitative analysis, all data sets were anonymized by randomization and two readers reviewed all the images using PACS. Two readers with 4 years of experience in breast imaging and 2 years of fellowship performed independent analyses of all $cDWI_{800}$, $cDWI_{1500}$, $sDWI_{1000}$, and $sDWI_{1500}$ images to evaluate the quality from the perspective of diagnostic feasibility. Qualitative analysis of each image set was evaluated using the following items: 1) degree of normal glandular tissue suppression, 2) overall image quality, and 3) lesion conspicuity. The scoring was performed using a 4-point Likert scale. It was adapted from a study by Dogan et al. (Table 2) (26). For calculating the cancer detection rate (CDR), lesion conspicuity score 1 was considered a negative examination, while lesion conspicuity score ≥ 2 was considered a positive examination. The lesion identified by the reader had to match the pathological location of the index lesion in order to constitute a true-positive result.

For quantitative analysis, two readers reviewed the information from all DWI sets of each patient and detected cancer with reference to the results of histopathological examination, T2-weighted images (T2WIs), and DCE T1-weighted images (DCE-MRI). The readers identified the index lesions on each DWI as a focal area of increased SI corresponding to the pathological location of the index lesion. Subsequently, a region of interest (ROI) was manually traced just within the outer margin of the identified abnormality on each image set, avoiding hemorrhage, necrosis, or cystic components. If no lesion could be identified on a given image set, an ROI was manually traced to correspond to the location of the identified lesion on other image sets. Five patients in

Table 2. Scales for Qualitative Analysis

Score	Normal Glandular Tissue Suppression	Overall Image Quality	Lesion Conspicuity
4	Uniform throughout field of view	Best	Very confidently assessed
3	Inhomogeneity present, but not preventing assessment	Fair	Confidently assessed but slightly lack of delineation of lesion margin
2	Inhomogeneity affects clinical assessment	Poor	Lesion present, features indeterminate
1	Inhomogeneity prevents diagnostic evaluation	Nondiagnostic	Nondiagnostic

https://doi.org/10.3348/kjr.2019.0568

Korean Journal of Radiology
KJR

whom the lesion could not be identified on any of the DWI sets were excluded from this quantitative analysis. For the remaining 45 patients, a small ROI was also traced in the normal glandular tissue of the contralateral breast, showing the densest normal breast parenchyma with homogeneous SI on all image sets as well as on T2WI. The mean value for each ROI was recorded. For each image set, cancer-to-parenchyma contrast ratio was calculated using the formula $(SI_G - SI_{cancer}) / (SI_G + SI_{cancer})$, where SI_{cancer} and SI_G were the average SIs for the cancer and normal glandular tissue, respectively (27, 28). ROI measurement was performed using a commercial workstation (AW Server 3.2, GE Healthcare). While assessing the SIs for cancer (mean size, 217 mm^2; range, 27–768 mm^2) and glandular tissue (mean size, 82 mm^2; range, 6–240 mm^2), the ROIs were first localized on $cDWI_{1500}$. The size, shape, and location of the ROIs were kept constant for all DWI sets in each patient by applying the copy-and-paste function on the monitor.

Statistical Analyses

The data were tested for normal distribution with Kolmogorov-Smirnov test. Continuous variables were expressed as mean ± standard deviation (SD). The mean values of the readers' ratings in the qualitative analysis were not directly compared, as these values were not strictly continuous variables. However, we decided to present a summary for DWI sets, expressed as mean ± SD. The average scores from the two readers for each image set were calculated and compared using the Friedman test with post-hoc analysis. Cancer-to-parenchyma contrast ratios on each image set were compared using one-way analysis of variance and post-hoc Tukey's test. Cochran's Q Test was used to compare DWI sets in terms of CDR. A p-value < 0.05 was considered statistically significant. Interobserver agreement in qualitative analysis was compared by percent agreement. Intraclass correlation coefficient (ICC) with a two-way random model of consistency was used to investigate interobserver agreement in the quantitative analysis (29). All statistical analyses were performed using SPSS Statistics version 24.0 (IBM Corp., Armonk, NY, USA).

RESULTS

Qualitative and Quantitative Analyses: All DWI Sets

Table 3 shows the scores assigned by the two readers for the qualitative analyses of all image sets. There were significant differences in the scores for suppression of normal glandular tissue, overall image quality, and lesion conspicuity among the four sets. All these parameters showed a tendency to increase with increasing b-value (p < 0.001). In the post-hoc analysis for suppression of normal glandular tissue, $sDWI_{1500}$ and $cDWI_{1500}$ showed significantly higher scores than $cDWI_{800}$ and $sDWI_{1000}$ (p < 0.001). $cDWI_{1500}$ showed significantly higher scores for the overall image quality than other DWI sets (p < 0.05). $sDWI_{1500}$ and $cDWI_{1500}$ showed significantly better lesion conspicuity than DWI sets with lower b-values (p < 0.001), whereas comparison between $sDWI_{1500}$ and $cDWI_{1500}$ revealed no significant difference (p > 0.05). There was no significant difference in any of the parameters between $sDWI_{1000}$ and

Table 3. Comparative Results of Qualitative and Quantitative Analyses between $cDWI_{800}$, $sDWI_{1000}$, $sDWI_{1500}$, and $cDWI_{1500}$

Parameters	$cDWI_{800}$	$sDWI_{1000}$	$sDWI_{1500}$	$cDWI_{1500}$	P	P*	$P^{\dagger}$	$P^{\ddagger}$	$P^{\S}$
Suppression of normal glandular tissue	2.34 ± 0.79	2.66 ± 0.78	3.32 ± 0.90	3.66 ± 0.78	< 0.001	< 0.001	< 0.001	< 0.001	< 0.001
Overall image quality	3.31 ± 0.88	3.33 ± 0.84	3.35 ± 0.81	3.73 ± 0.62	< 0.001	> 0.999	0.002	> 0.999	0.002
Lesion conspicuity	2.83 ± 0.96	3.09 ± 0.94	3.52 ± 0.92	3.39 ± 0.90	< 0.001	< 0.001	< 0.001	< 0.001	0.051
CDR (invasive and *in situ* cancer), %	84.0 (42/50)	86.0 (43/50)	90.0 (45/50)	90.0 (45/50)	0.061				
CDR (invasive cancer), %	89.7 (35/39)	92.3 (36/39)	94.9 (37/39)	94.9 (37/39)	0.194				
Cancer-to-parenchyma contrast ratio	0.47 ± 0.17	0.54 ± 0.16	0.63 ± 0.17	0.55 ± 0.18	< 0.001	< 0.001	0.009	0.004	0.961

Pooled data from two readers are mean ± standard deviation. P values were calculated using Friedman test for qualitative anlaysis, Cochran's Q Test for CDR, and one-way ANOVA for cancer-to-parenchyma contrast ratio. *p values indicate comparisons between $cDWI_{800}$ and $sDWI_{1500}$ in post-hoc analysis, $^{\dagger}p$ values indicate comparisons between $cDWI_{800}$ and $cDWI_{1500}$ in post-hoc analysis, $^{\ddagger}p$ values indicate comparisons between $sDWI_{1000}$ and $sDWI_{1500}$ in post-hoc analysis, $^{\S}p$ values indicate comparisons between $sDWI_{1000}$ and $cDWI_{1500}$ in post-hoc analysis. CDR = cancer detection rate, $cDWI_{800}$ = conventional low b-value (800 s/mm^2) diffusion-weighted imaging, $cDWI_{1500}$ = conventional high b-value (1500 s/mm^2) diffusion-weighted imaging, $sDWI_{1000}$ = synthetic high b-value (1000 s/mm^2) diffusion-weighted imaging, $sDWI_{1500}$ = synthetic high b-value (1500 s/mm^2) diffusion-weighted imaging

https://doi.org/10.3348/kjr.2019.0568

$cDWI_{800}$ in qualitative analysis. CDR was not significantly different among the four DWI sets ($p = 0.061$ for all cancers and $p = 0.194$ for invasive cancers) (Table 3).

In five patients (5/50), cancers could not be identified on any of the DWI sets. The histopathological diagnoses of these lesions included one tubular carcinoma (pathologic size: 1.2 cm), one invasive carcinoma of no special type (0.6 cm), and three ductal carcinomas *in situ* (1–2.8 cm).

The cancer-to-parenchyma contrast ratios in the remaining 45 patients showed a significant difference among the four DWI sets ($p < 0.001$). $sDWI_{1500}$ revealed significantly higher cancer-to-parenchyma contrast ratios than the other DWI sets in the post-hoc analysis ($p < 0.05$). Interobserver agreement of the cancer-to-parenchyma contrast ratios of all image sets was excellent (ICC: 0.887–0.960, $p < 0.001$).

Qualitative and Quantitative Analyses: $cDWI_{1500}$ vs. $sDWI_{1500}$

The two readers assigned a score of more than 3 points to all parameters on both $cDWI_{1500}$ and $sDWI_{1500}$, implying that both these sets were "fair for diagnostic use" (Table 4). The mean scores for suppression of normal glandular tissue and overall image quality were significantly higher in $cDWI_{1500}$ than in $sDWI_{1500}$ (reader 1, 3.56 and 3.86 vs. 3.14 and 3.42, respectively; and reader 2, 3.76 and 3.60 vs. 3.50 and 3.28, respectively; $p < 0.05$). However, lesion conspicuity scores were higher in $sDWI_{1500}$ than in $cDWI_{1500}$ (reader 1, 3.54 vs. 3.44, respectively; and reader 2, 3.50 vs. 3.34, respectively; $p < 0.05$). Fair to good interobserver agreement was observed in qualitative analysis of $sDWI_{1500}$ and $sDWI_{1500}$ (range: 44.0–72.0%).

Both readers showed similar CDR values in $sDWI_{1500}$ and $cDWI_{1500}$ for all cancers (reader 1, 90.0% [45/50]; and reader 2, 94.0% [47/50]) and for invasive cancers (reader 1, 94.9% [37/39]; and reader 2, 100% [39/39]) (Table 5). DCE-MRI demonstrated the best CDR (for all cancers, reader 1 and 2, 96.0% [48/50] and for invasive cancers; reader 1 and 2, 100% [39/39]). However, there was no significant difference in CDR among $sDWI_{1500}$, $cDWI_{1500}$, and DCE-MRI ($p \geq 0.05$).

The cancer-to-parenchyma contrast ratios described by the two readers were significantly greater in $sDWI_{1500}$ (0.62 ± 0.18 and 0.63 ± 0.17) than in $cDWI_{1500}$ (0.55 ± 0.18 and 0.55 ± 0.18) ($p < 0.001$). Representative cases are shown in Figure 1.

DISCUSSION

In the present study, sDWI provided better lesion conspicuity and cancer-to-parenchyma contrast ratios than cDWI at the same high b-value (1500 s/mm^2). CDR values were comparable between these two sets. Although $sDWI_{1500}$ showed inferior normal breast tissue suppression and overall image quality than $cDWI_{1500}$, $sDWI_{1500}$ yielded better scores in qualitative analysis than DWI sets with lower b-values. These results indicate that sDWI can be a feasible option for the diagnosis of breast cancer.

Table 4. Comparative Results of Qualitative Analysis between $cDWI_{1500}$ and $sDWI_{1500}$

Parameters	Readers	$cDWI_{1500}$	Percent Agreement (%)	$sDWI_{1500}$	Percent Agreement (%)	*P*
Suppression of normal glandular tissue	1	3.56 ± 0.91	72.0	3.14 ± 0.95	56.0	< 0.001
	2	3.76 ± 0.62		3.50 ± 0.81		< 0.001
Overall image quality	1	3.86 ± 0.50	70.0	3.42 ± 0.70	44.0	< 0.001
	2	3.60 ± 0.70		3.28 ± 0.90		0.002
Lesion conspicuity	1	3.44 ± 0.97	68.0	3.54 ± 0.97	64.0	0.025
	2	3.34 ± 0.82		3.50 ± 0.86		0.046

Data are mean ± standard deviation. *P* values were calculated using Wilcoxon signed rank test.

Table 5. Comparison of CDR and Quantitative Analysis between $cDWI_{1500}$ and $sDWI_{1500}$

Parameters	Readers	$cDWI_{1500}$ (%)	$sDWI_{1500}$ (%)	DCE-MRI (%)	*P*
CDR (invasive and *in situ* cancer)	1	90.0 (45/50)	90.0 (45/50)	96.0 (48/50)	0.050
	2	94.0 (47/50)	94.0 (47/50)	96.0 (48/50)	0.368
CDR (invasive cancer)	1	94.9 (37/39)	94.9 (37/39)	100 (39/39)	0.135
	2	100 (39/39)	100 (39/39)	100 (39/39)	1.000
Cancer-to-parenchyma contrast ratio	1	0.55 ± 0.18	0.62 ± 0.18	NA	< 0.001
	2	0.55 ± 0.18	0.63 ± 0.17	NA	< 0.001

DCE-MRI = dynamic contrast-enhanced MRI, NA = not applicable

https://doi.org/10.3348/kjr.2019.0568

Korean Journal of Radiology
KJR

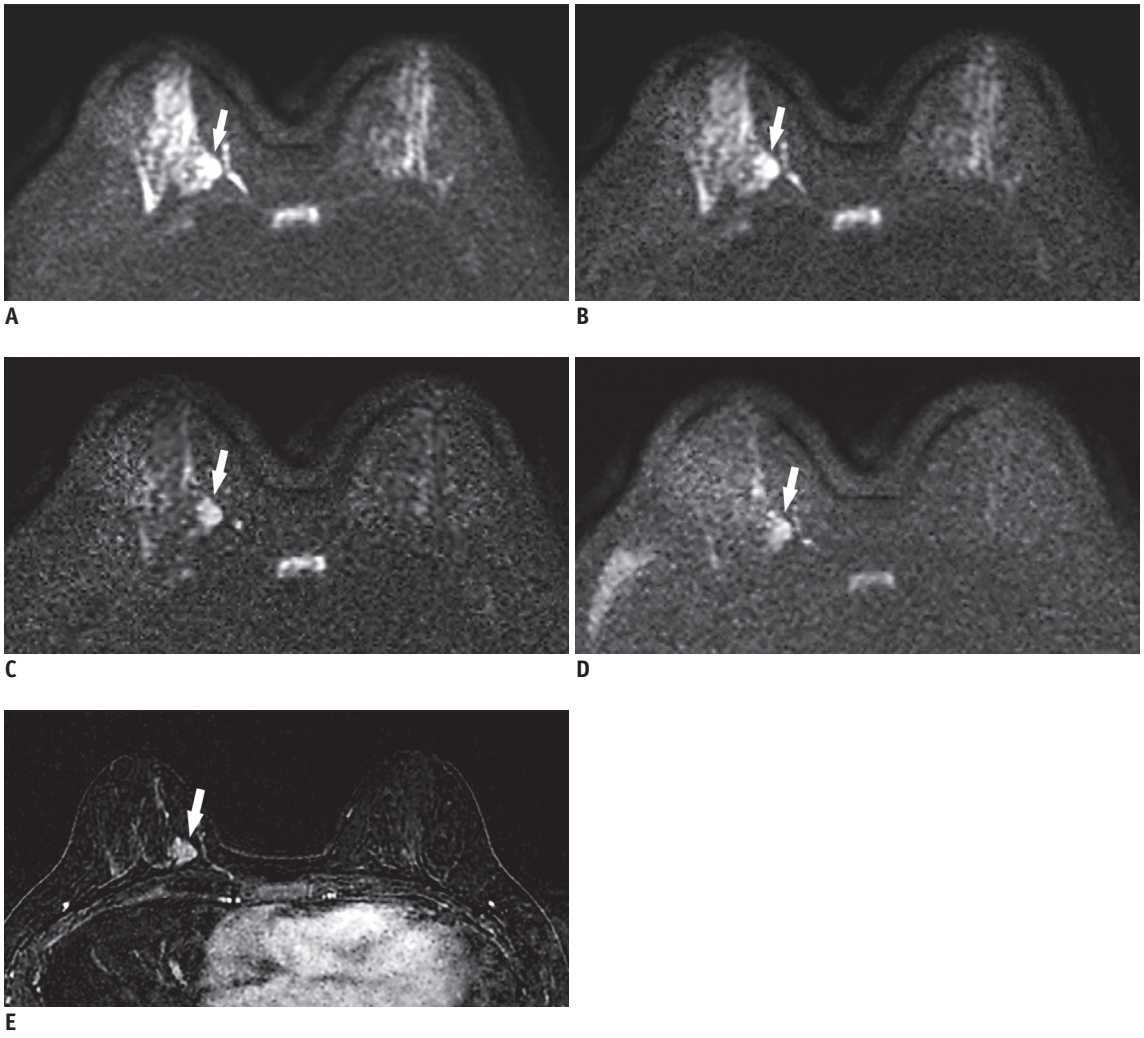

Fig. 1. 49-year-old woman with 2.4 cm invasive ductal carcinoma (histologic grade 2) in right 3 o'clock position.
On conventional axial DWI at b-value of 800 s/mm^2 **(A)** and on synthetic DWI at b-value of 1000 s/mm^2 **(B)**, breast cancer (arrows) shows hyperintensity, but border is obscured by insufficiently suppressed normal glandular tissue [suppression of normal glandular tissue: 2, image quality: 3, lesion conspicuity: 2, and cancer-to-parenchyma contrast ratios: 0.33 for **(A)** and 0.37 for **(B)**]. On synthetic DWI at b-value of 1500 s/mm^2 **(C)**, cancer (arrows) is clearly seen (suppression of normal glandular tissue: 3, image quality: 3, lesion conspicuity: 4, and cancer-to-parenchyma contrast ratio: 0.45) when compared with conventional DWI at b-value of 1500 s/mm^2 **(D)** (suppression of normal glandular tissue: 3, image quality: 3, lesion conspicuity: 3, and cancer-to-parenchyma contrast ratio: 0.39). **(E)** Axial post-contrast subtraction image at same slice location demonstrates the enhancing tumor (arrow), showing similar lesion visibility on synthetic DWI at b-value of 1500 s/mm^2. DWI = diffusion-weighted imaging

Theoretically, an increase in the b-values should increase background suppression, resulting in better lesion conspicuity. Accordingly, suppression of glandular tissue, overall image quality, and lesion conspicuity improved in the present study with an increase in the b-value. Lesion conspicuity received the best score in $sDWI_{1500}$. This could be explained by the higher cancer-to-parenchyma contrast ratio in $sDWI_{1500}$ than in other DWI sets. This result is consistent with the results of previous studies involving malignancies of prostate, pancreas, and uterine cervix that demonstrated higher contrast ratios between the malignant tumor and the normal tissue on sDWI with increasing b-values (9, 13, 16, 21, 22). Recently, Bickel et al. (30) demonstrated changes in the parameters on sDWI at different b-values (1000–2000 s/mm^2) in patients with breast cancer. They demonstrated a decrease in relative SNRs and contrast-to-noise ratios with increasing b-values, whereas cancer-to-parenchyma contrast ratios increased significantly (30). In the present study, cancer-to-parenchyma contrast ratios were greater in $sDWI_{1500}$ than in $cDWI_{1500}$. At a b-value of 1500 s/mm^2, the SI of the background tissue began fading significantly, allowing better lesion conspicuity. However, the SI of

https://doi.org/10.3348/kjr.2019.0568

cancer was also suppressed in cDWI. In contrast, the SI of cancer was not suppressed in sDWI, yielding higher cancer-to-parenchyma contrast ratios. Similar results have been reported in previous studies on pancreatic cancer (b-values: 1500 and 2000 s/mm^2) and prostate cancer (b-value: 1500 s/mm^2), showing better cancer-to-parenchyma contrast ratios in sDWI than in cDWI at the same b-value (9, 13).

In the current study, $cDWI_{1500}$ and $sDWI_{1500}$ showed better background suppression of normal tissue and comparable image quality when compared with DWI sets with lower b-values. This finding was consistent with the findings of previous studies on sDWI with high b-values (1500–2500 s/mm^2) (23, 25). In addition, there was no significant difference in background suppression of normal tissue between $cDWI_{1500}$ and $sDWI_{1500}$. However, the image quality in $sDWI_{1500}$ was inferior to that in $cDWI_{1500}$. Lower readers' ratings for image quality on $sDWI_{1500}$ might be attributed to the granular appearance of the image, which may be considered an inevitable artifact of synthetic images derived from ADC. Nevertheless, the granular appearance on sDWI did not interfere with the detection of cancers. Thus, the overall image quality of sDWI might be acceptable for clinical use.

The image quality of DWI is affected by b-value selection. A previous meta-analysis recommended b-values of 0 and 1000 s/mm^2 on 1.5T MRI for optimal differentiation between benign and malignant lesions (31). To date, there are no meta-analysis reports on the most appropriate b-value for 3T MRI. Moreover, detectability of breast cancer on DWI may be affected by patient-related factors. Hahn et al. (32) reported that detectability of invasive breast cancer on DWI was not influenced by background parenchymal enhancement, mammographic density, menopausal status, or menstrual cycle, but it was influenced by the degree of background signal suppression. However, Bickel et al. (30) reported that the preferred b-value on sDWI was commonly between 1200 and 1600 s/mm^2 in the low breast density group and between 1400 and 1600 s/mm^2 in the high breast density group. In the present study, insufficient suppression of normal fibroglandular tissue was commonly seen in younger premenopausal patients (median age < 52.5 years) with high breast density, which can result in failure to detect breast cancer on DWI. Considering these issues, optimal b-value may vary according to patient-related factors. However, obtaining images at multiple b-values is time-consuming. In this regard, sDWI can be a solution to overcome the limitations. sDWI using MAGiC DWI can provide synthetic images of comparable quality that can be acquired in 5 seconds, as opposed to 4–5 minutes for cDWI. However, further studies are needed to validate these claims, as several other software are available to generate sDWI.

This study has some limitations that should be considered when interpreting the findings. This study was retrospective in nature, had a single-center design, and limited sample size. Breast MRI at our institution is mainly performed in patients with suspected breast cancer. Therefore, our sample selection was biased, considering the absence of other breast pathologies. All patients underwent MRI using a specific 3T scanner. Recent studies are exploring the application of DWI using various magnetic resonance scanners and software including different approaches to fat suppression or the readout-segmented EPI technique, which may affect the obtained images. Our analysis of cancer-to-parenchyma contrast ratios was based on assessment of the index lesion rather than the assessment of the complete tumor foci. Moreover, manual ROI selection was reader-dependent and small in size, which may have affected the results despite interobserver agreement. Relatively low cancer-to-parenchyma contrast ratios of DWI sets might be induced by the inhomogeneity of SI, which may have affected the results. We considered percent agreement to evaluate interobserver agreement instead of kappa statistics, as kappa statistics provide paradoxically low values due to imbalance in the number of concordant and discordant pairs (33, 34).

In conclusion, $sDWI_{1500}$ provided CDR comparable to $cDWI_{1500}$ in patients with breast cancer. It also showed better lesion conspicuity and higher cancer-to-parenchyma contrast ratios than $cDWI_{1500}$. Therefore, sDWI can be a feasible MRI option for screening or preoperative evaluation of patients with breast cancer due to its inherent benefits such as rapid scan time and reduced need for additional scanning or contrast agent. However, the overall image quality and background normal breast tissue suppression were inferior when compared with cDWI. Therefore, further technological efforts are essential to solve these issues and to expand the clinical use of sDWI in detecting breast cancer. We believe that further studies with larger sample sizes and various magnetic resonance scanners will validate our results.

Supplementary Materials

The Data Supplement is available with this article at

https://doi.org/10.3348/kjr.2019.0568

https://doi.org/10.3348/kjr.2019.0568.

Conflicts of Interest

The authors have no potential conflicts of interest to disclose.

ORCID iDs

Hye Jin Baek
https://orcid.org/0000-0001-7349-2841
Bo Hwa Choi
https://orcid.org/0000-0001-7276-1579
Ji Young Ha
https://orcid.org/0000-0001-5769-3045
Kyeong Hwa Ryu
https://orcid.org/0000-0003-1599-8881
Jin Il Moon
https://orcid.org/0000-0002-5329-1767
Sung Eun Park
https://orcid.org/0000-0002-2832-8900
Kyungsoo Bae
https://orcid.org/0000-0002-2545-2682
Kyung Nyeo Jeon
https://orcid.org/0000-0003-2267-0366
Eun Jung Jung
https://orcid.org/0000-0001-8413-613X

REFERENCES

1. Liberman L, Morris EA, Lee MJ, Kaplan JB, LaTrenta LR, Menell JH, et al. Breast lesions detected on MR imaging: features and positive predictive value. *AJR Am J Roentgenol* 2002;179:171-178
2. Kuhl CK, Schrading S, Strobel K, Schild HH, Hilgers RD, Bieling HB. Abbreviated breast magnetic resonance imaging (MRI): first postcontrast subtracted images and maximum-intensity projection—A novel approach to breast cancer screening with MRI. *J Clin Oncol* 2014;32:2304-2310
3. Chen X, Li WL, Zhang YL, Wu Q, Guo YM, Bai ZL. Meta-analysis of quantitative diffusion-weighted MR imaging in the differential diagnosis of breast lesions. *BMC Cancer* 2010;10:693
4. Zhang L, Tang M, Min Z, Lu J, Lei X, Zhang X. Accuracy of combined dynamic contrast-enhanced magnetic resonance imaging and diffusion-weighted imaging for breast cancer detection: a meta-analysis. *Acta Radiol* 2016;57:651-660
5. Trimboli RM, Verardi N, Cartia F, Carbonaro LA, Sardanelli F. Breast cancer detection using double reading of unenhanced MRI including T1-weighted, T2-weighted STIR, and diffusion-weighted imaging: a proof of concept study. *AJR Am J Roentgenol* 2014;203:674-681
6. Yabuuchi H, Matsuo Y, Sunami S, Kamitani T, Kawanami S, Setoguchi T, et al. Detection of non-palpable breast cancer in asymptomatic women by using unenhanced diffusion-weighted and T2-weighted MR imaging: comparison with mammography and dynamic contrast-enhanced MR imaging. *Eur Radiol* 2011;21:11-17
7. Woodhams R, Inoue Y, Ramadan S, Hata H, Ozaki M. Diffusion-weighted imaging of the breast: comparison of b-values 1000 s/mm^2 and 1500 s/mm^2. *Magn Reson Med* Sci 2013;12:229-234
8. Blackledge MD, Leach MO, Collins DJ, Koh DM. Computed diffusion-weighted MR imaging may improve tumor detection. *Radiology* 2011;261:573-581
9. Fukukura Y, Kumagae Y, Hakamada H, Shindo T, Takumi K, Kamimura K, et al. Computed diffusion-weighted MR imaging for visualization of pancreatic adenocarcinoma: comparison with acquired diffusion-weighted imaging. *Eur J Radiol* 2017;95:39-45
10. Gatidis S, Schmidt H, Martirosian P, Nikolaou K, Schwenzer NF. Apparent diffusion coefficient-dependent voxelwise computed diffusion-weighted imaging: an approach for improving SNR and reducing T2 shine-through effects. *J Magn Reson Imaging* 2016;43:824-832
11. Shimizu H, Isoda H, Fujimoto K, Kawahara S, Furuta A, Shibata T, et al. Comparison of acquired diffusion weighted imaging and computed diffusion weighted imaging for detection of hepatic metastases. *Eur J Radiol* 2013;82:453-458
12. Kawahara S, Isoda H, Fujimoto K, Shimizu H, Furuta A, Arizono S, et al. Additional benefit of computed diffusion-weighted imaging for detection of hepatic metastases at 1.5T. *Clin Imaging* 2016;40:481-485
13. Rosenkrantz AB, Chandarana H, Hindman N, Deng FM, Babb JS, Taneja SS, et al. Computed diffusion-weighted imaging of the prostate at 3 T: impact on image quality and tumour detection. *Eur Radiol* 2013;23:3170-3177
14. Ueno Y, Takahashi S, Kitajima K, Kimura T, Aoki I, Kawakami F, et al. Computed diffusion-weighted imaging using 3-T magnetic resonance imaging for prostate cancer diagnosis. *Eur Radiol* 2013;23:3509-3516
15. Maas MC, Fütterer JJ, Scheenen TW. Quantitative evaluation of computed high B value diffusion-weighted magnetic resonance imaging of the prostate. *Invest Radiol* 2013;48:779-786
16. Bittencourt LK, Attenberger UI, Lima D, Strecker R, de Oliveira A, Schoenberg SO, et al. Feasibility study of computed vs measured high b-value (1400 s/mm^2) diffusion-weighted MR images of the prostate. *World J Radiol* 2014;6:374-380
17. Vural M, Ertaş G, Onay A, Acar Ö, Esen T, Sağlıcan Y, et al. Conspicuity of peripheral zone prostate cancer on computed diffusion-weighted imaging: comparison of $cDWI_{1500}$, $cDWI_{2000}$, and $cDWI_{3000}$. *Biomed Res Int* 2014;2014:768291
18. Ueno Y, Takahashi S, Ohno Y, Kitajima K, Yui M, Kassai Y, et al. Computed diffusion-weighted MRI for prostate cancer

detection: the influence of the combinations of b-values. *Br J Radiol* 2015;88:20140738
19. Grant KB, Agarwal HK, Shih JH, Bernardo M, Pang Y, Daar D, et al. Comparison of calculated and acquired high b value diffusion-weighted imaging in prostate cancer. *Abdom Imaging* 2015;40:578-586
20. Rosenkrantz AB, Parikh N, Kierans AS, Kong MX, Babb JS, Taneja SS, et al. Prostate cancer detection using computed very high b-value diffusion-weighted imaging: how high should we go? *Acad Radiol* 2016;23:704-711
21. Verma S, Sarkar S, Young J, Venkataraman R, Yang X, Bhavsar A, et al. Evaluation of the impact of computed high b-value diffusion-weighted imaging on prostate cancer detection. *Abdom Radiol (NY)* 2016;41:934-945
22. Moribata Y, Kido A, Fujimoto K, Himoto Y, Kurata Y, Shitano F, et al. Feasibility of computed diffusion weighted imaging and optimization of b-value in cervical cancer. *Magn Reson Med Sci* 2017;16:66-72
23. O'Flynn EA, Blackledge M, Collins D, Downey K, Doran S, Patel H, et al. Evaluating the diagnostic sensitivity of computed diffusion-weighted MR imaging in the detection of breast cancer. *J Magn Reson Imaging* 2016;44:130-137
24. Park JH, Yun B, Jang M, Ahn HS, Kim SM, Lee SH, et al. Comparison of the diagnostic performance of synthetic versus acquired high b-value (1500 s/mm^2) diffusion-weighted MRI in women with breast cancers. *J Magn Reson Imaging* 2019;49:857-863
25. Zhou J, Chen E, Xu H, Ye Q, Li J, Ye S, et al. Feasibility and diagnostic performance of voxelwise computed diffusion-weighted imaging in breast cancer. *J Magn Reson Imaging* 2019;49:1610-1616
26. Dogan BE, Ma J, Hwang K, Liu P, Yang WT. T1-weighted 3D dynamic contrast-enhanced MRI of the breast using a dual-echo Dixon technique at 3 T. *J Magn Reson Imaging* 2011;34:842-851
27. Cornfeld DM, Israel G, McCarthy SM, Weinreb JC. Pelvic imaging using a T1W fat-suppressed three-dimensional dual echo Dixon technique at 3T. *J Magn Reson Imaging* 2008;28:121-127
28. Hori M, Kim T, Onishi H, Ueguchi T, Tatsumi M, Nakamoto A, et al. Uterine tumors: comparison of 3D versus 2D T2-weighted turbo spin-echo MR imaging at 3.0 T—Initial experience. *Radiology* 2011;258:154-163
29. Lin LI. A concordance correlation coefficient to evaluate reproducibility. *Biometrics* 1989;45:255-268
30. Bickel H, Polanec SH, Wengert G, Pinker K, Bogner W, Helbich TH, et al. Diffusion-weighted MRI of breast cancer: improved lesion visibility and image quality using synthetic b-values. *J Magn Reson Imaging* 2019;50:1754-1761
31. Dorrius MD, Dijkstra H, Oudkerk M, Sijens PE. Effect of b value and pre-admission of contrast on diagnostic accuracy of 1.5-T breast DWI: a systematic review and meta-analysis. *Eur Radiol* 2014;24:2835-2847
32. Hahn SY, Ko ES, Han BK, Lim Y, Gu S, Ko EY. Analysis of factors influencing the degree of detectability on diffusion-weighted MRI and diffusion background signals in patients with invasive breast cancer. *Medicine (Baltimore)* 2016;95:e4086
33. Viera AJ, Garrett JM. Understanding interobserver agreement: the kappa statistic. *Fam Med* 2005;37:360-363
34. Feinstein AR, Cicchetti DV. High agreement but low kappa: I. The problems of two paradoxes. *J Clin Epidemiol* 1990;43:543-549

https://doi.org/10.3348/kjr.2019.0568